

Directed Broadcast with Overhearing for Sensor Networks

Raja Jurdak
CSIRO ICT Centre
and

Antonio G. Ruzzelli, Gregory M. P. O'Hare
School of Computer Science and Informatics
University College Dublin

and
Russell Higgs
School of Mathematical Science
University College Dublin

The efficient management of scarce network resources, including energy and bandwidth, represents a central challenge for wireless sensor networks. The current trend in resource management relies on the introduction of control mechanisms, such as control message exchanges, node-specific addressing, and storage of partial network state information. These mechanisms typically incur communication and processing overhead that does not scale well for larger or denser networks. Instead of introducing control mechanisms for network resource management, this article proposes and evaluates a directed broadcast with overhearing (DBO) approach for sensor networks that combines directed broadcast at the network layer with CSMA and packet overhearing at the MAC layer. Through avoidance of control messaging and exchange of network state information, DBO trades off limited packet duplication overhead for control messaging overhead. This article introduces an analytical model that provides the basis for DBO evaluation and for analysis of the approach's transient packet re-transmissions, route convergence, and energy consumption in the average and worst cases. We also present the model implementation details and the simulation experiments that explore the suitability of DBO for networks of different sizes with three different radio models that vary the width of grey regions, and we compare DBO's energy consumption against conventional unicast beacon-based and snooping-based routing protocols. The results indicate that that DBO's route convergence requires an average of five hops for ideal radio reception, seven hops for narrow grey regions, and twelve hops for wide grey regions. These results confirm that DBO shifts energy consumption from critical nodes near the base station to nodes near the source. The overall energy consumption of limited packet duplication overhead with DBO compared to unicast routing shrinks for medium to large size networks, rendering it more favorable than conventional communication approaches for large and dense sensor networks.

Categories and Subject Descriptors: C.2.2 [**Computer-Communications Networks**]: Network Protocols; C.2.1 [**Computer-Communications Networks**]: Network Architecture and Design
General Terms: Design, Management, Theory, Algorithms, Performance

Author's address: QCAT Technology Court Pullenvale QLD 4069 Australia.

Permission to make digital/hard copy of all or part of this material without fee for personal or classroom use provided that the copies are not made or distributed for profit or commercial advantage, the ACM copyright/server notice, the title of the publication, and its date appear, and notice is given that copying is by permission of the ACM, Inc. To copy otherwise, to republish, to post on servers, or to redistribute to lists requires prior specific permission and/or a fee.

© 2010 ACM 0000-0000/2010/0000-0001 \$5.00

Additional Key Words and Phrases: Cross-layer, architecture, sensor networks, protocols, directed broadcast, overhearing

1. INTRODUCTION

The reliance of wireless sensor networks on small battery-operated nodes requires scalable and efficient strategies for resource management in large networks. The ever shrinking form factor of sensor nodes is one of the main limiting factors for the available energy resources in the network. Miniaturization of processors, memory, and sensors has far outpaced improvements in battery technology, which further highlights the importance of energy efficiency in sensor networks.

A considerable class of bandwidth-limited sensor networks requires efficient use of the available channel resources in addition to the design goal of energy efficiency. The bandwidth limitation of these networks stems from their physical layer characteristics. For example, networks that employ acoustic [Jurdak et al. 2006] or infrared [Gonzalez-Velazquez et al. 2002] links have inherently low available bandwidth. Even in certain RF networks [Rangwala et al. 2006], the ambient interference in a harsh deployment environment can cause degradation of the signal-to-noise ratio (SNR), forcing the use of low bit rates for communication.

Conventional communication protocols for sensor networks introduce control mechanisms, such as messaging sequences, per-node addresses, and network state storage, in order to limit energy consumption in the network. While these mechanisms generally incur a communication overhead, their energy savings outweigh their overhead for specific network scenarios. One shortcoming of conventional protocols is that they are not suitable for bandwidth-limited networks, which cannot afford the communication overhead of control messages. Furthermore, conventional mechanisms do not scale well in dense and large networks, as the network-wide overhead of control messaging, state storage, and addressing grows significantly for large scale sensor networks. Mobile node scenarios and low duty cycle networks further highlight the scalability issues relating to conventional control mechanisms.

Recent studies have shown that mechanisms with low control overhead provide a viable alternative for large scale networks [Akkaya and Younis 2005]. However, these studies have investigated the benefits of a low overhead mechanism at a single communication layer in isolation of other layers. Cross-layer design, which increases the level of coordination and interaction between communication layers, has received increasing recognition as an efficient resource management design strategy for sensor networks [Jurdak 2007]. An extreme cross-layer design approach is to holistically design two or more layers, resulting in the complete integration of functionalities of the layers. This paper proposes a holistic cross-layer approach, called directed broadcast with overhearing (DBO), that combines directed broadcast from the network layer, and packet overhearing in CSMA-based networks at the MAC layer, in order to provide both energy and bandwidth efficiency in medium to large scale sensor networks. The main concept of DBO is that *less* control messaging (such as RTS/CTS, hello messages, etc.), state storage (such as routing costs), and addressing (which incurs a constant overhead per packet), can yield *more* energy and bandwidth efficiency in dense and large scale sensor networks. DBO reduces control

mechanisms that manage packet delivery from source nodes towards the data sink.

In DBO, nodes learn their minimum hop count, or more generally their minimum path cost, from the nearest data sink progressively through overhearing neighbor's packets during an initial phase. After the initial phase, nodes can simply broadcast their data packets, which include the hop zone of the source node. Through directed broadcast communication, only the nodes that are at a closer hop zone to the base station will forward the packet. Any node that overhears a packet transmission from its own hop zone refrains from forwarding the packet, which represents a form of intelligent filtering. The absence of any addressing or state storage can cause transient packet duplication in the process of forwarding data from source to sink, because nodes that are out of each other's transmission range may independently forward the same packet along different paths. However, our analysis and comprehensive simulations by which we study the effect of *route convergence*¹ in data collection of a dense sensor network show that the communication and energy overhead of DBO is small for medium to large networks.

The novel contributions of this article are fourfold:

- (1) Proposal of a holistic approach that combines directed broadcast and packet overhearing for curbing the use of other control mechanisms.
- (2) Development of an analytical system model to investigate the route convergence behavior of DBO.
- (3) Implementation of the analytical model and presentation of comprehensive simulation results for exploring the energy impact of packet duplication and for identifying the beneficial scenarios for DBO under 3 different radio models that vary the width of the grey regions of intermittent connectivity around a sender.
- (4) Comparison of the energy consumption of DBO against beacon-based and snooping-based unicast routing protocols.

The remainder of the paper is structured as follows. Section 2 surveys the related literature. Section 3 introduces the analytical model that provides the basis for DBO, and provides an analysis of the route convergence for DBO packet transmissions. Section 4 presents the model implementation details and the simulations that explore the suitability of DBO for networks of different sizes, under 3 radio models, and based on communication and energy overhead considerations. Finally, section 5 discusses the results and concludes the paper.

2. RELATED WORK

In sensor networks, the broadcast nature of the wireless channel causes all neighbors of the sender to overhear packets, resulting in unnecessary expenditure of node energy [Basu and Redi 2004]. Packet overhearing is more accentuated in synchronous CSMA protocols, such as SMAC [Ye et al. 2004] and TMAC [Dam and Langendoen 2003], in which all nodes in a neighborhood wake-up simultaneously to listen to incoming packets. Enabling asynchronous node duty cycles effectively mitigates energy consumption due to overhearing. For example BMAC [Polastre et al. 2004] and

¹What we mean by route convergence is the number of hops and the number of packet duplicates before there is only a single data packet transmission per hop.

WISEMAC [El-Hoiydi and Decotignie 2004] decrease packet overhearing through a mechanism of asynchronous low power listening (LPL). The effectiveness of LPL has also been studied in [Halkes et al. 2005]. A drawback of BMAC and WISEMAC is their poor performance under high contention scenarios due to the usage of a long wake-up preamble. For high channel contention, several nodes may transmit their wake-up preamble consecutively to neighboring nodes. The partially overlapping preambles can prevent the transmission of the actual data. Asynchronous transmission approaches mitigate the problem of energy consumption due to idle listening by shifting it from the receiver to the transmitter. This is advantageous only if the network data-rate is low. Otherwise, low power listening can cause significant packet latency. Rhee et al. [Rhee et al. 2005] developed ZMAC that outperforms BMAC in high contention scenarios through a combination of TDMA and CSMA access. However, ZMAC still causes higher energy consumption for low contention scenarios.

Most existing sensor network MAC protocols couple low duty cycles with the RTS/CTS handshake, which causes high overhead due to the small size of data payloads in sensor networks. For instance, the control messages for MAC handshakes and headers in IEEE 802.15.4 [802.15.4 2003] is 52 bytes for RTS/CTS/header/ACK and 14 bytes for transmission without RTS/CTS handshake. As typical IEEE 802.15.4 packets have a payload of 100 bytes, the MAC overhead is 52% with RTS/CTS and 14% without it. Low duty cycle protocols can suffer from high packet latency that goes up to tens of seconds due to the unfavorable combination of node duty-cycling and multihop routing. Earlier studies [Ruzzelli et al. 2006] demonstrate that the combination of low duty cycle and on-demand routing, such as ESR [Wu et al. 2004] as a lightweight version of DSR [Johnson and Maltz 1996], can accumulate considerable packet delay and in some cases cause packet losses. A related study in [Das et al. 2001], had shown earlier that the end-to-end delay is greater for other reactive routing techniques, such as AODV, than it is for DSR.

Another drawback of conventional unicast protocols is that they require state information about neighboring nodes, such as the routing parent node's ID. Unicast approaches are not suitable in large scale, dynamic and mobile networks in which nodes can die over time, new nodes can join the network and others can have transient disconnections due to fluctuations in the channel conditions. Geographic routing protocols, such as [Zorzi and Rao 2003] and [Karp and Kung 2000], attempt to tackle addressing and scalability issues. Geographic routing typically requires the usage of localization techniques, where a few nodes have GPS receivers and the rest of nodes calculate their relative location through trilateration graphs [Eren et al. 2004] or through a probabilistic notion of robust quadrilaterals [Moore et al. 2004].

Tests on the signal quality of sensor networks [Zhou et al. 2004] demonstrated that low power signals of the nodes are prone to temporary link breaks due to a nearby sources of interference, such as a microwave oven or a moving object in the vicinity of the network. Zhao and Govindan [Zhao and Govindan 2003] independently confirmed the signal unreliability through experimental measurements that quantified the prevalence of gray areas and communication asymmetry. As such, transmitting to a single neighboring node may not provide sufficient reliabil-

ity for many applications. Similar empirical experiments by [Srinivasan et al. 2006] and [Cerpa et al. 2005] have also confirmed the existence of a grey region around a sensor node where packets may be dropped with a nearly random probability.

Broadcasting, which is the most naive solution for wireless communication, avoids node addressing and overcomes temporary disconnections by transmitting to all nodes in the neighborhood. Thus, in a dense network, intermittent connectivity and packet losses with some neighbors do not prevent other neighbors from receiving a packet and forwarding it if necessary. This inherently provides broadcasting with a higher degree of reliability than unicast, which relies on a single forwarder at each hop selected according to some cost metric. However, broadcasting causes redundant receptions and retransmissions of packets that, if not controlled, may lead to high number of collisions and contentions, as described in [Tseng et al. 2002]. In order to mitigate this issue, Ye et al. [Ye et al. 2001] developed a forwarding algorithm that utilizes minimum cost forwarding. Their technique decreases the number of re-transmissions by only allowing nodes with a smaller cost value than the transmitter to forward a packet. Minimum cost forwarding leaves an open definition of cost to enable customization of the routing cost to the performance requirements of different applications. However, the protocol can still cause many re-transmissions especially in dense network scenarios, and no qualitative or quantitative analysis of its overhead energy consumption is provided.

In the proposed DBO approach, we examine analytically the reduction of the number of re-transmissions by allowing nodes to overhear nearby transmissions through the CSMA mechanism. Nodes can then discard duplicate packets that are being forwarded by neighboring nodes. This obviously requires cross-layer interaction between MAC and routing protocols, as pointed out by [Woo et al. 2003], who emphasized the importance of link state and local neighborhood information. Information sharing among different communication layers has received a lot of attention recently as an effective optimization strategy for wireless sensor networks [Jurdak 2007][Melodia et al. 2005][Polastre et al. 2005]. For example, adaptive low power listening (ALPL) [Jurdak et al. 2007] is a recent cross-layer optimization over BMAC that enables each sensor node to locally set its duty on the basis of a cost function that includes metrics from several communication layers, for the purpose of balancing the load in the network. However, cross-layering must adhere to cautionary design rules so that it does not stifle further innovation and complicate system maintenance [Kawadia and Kumar 2005].

The DBO approach is a generalization of MERLIN [Ruzzelli et al. 2008] that adopts a holistic approach combining MAC and routing layer functionality, an extreme form of cross-layer design. In particular, DBO builds on MERLIN's division of the network into concentric timezones. MERLIN implements a holistic MAC/routing vision that addresses scheduling issues between timezones, packet concatenation and route maintenance. This study takes a step back from timing issues and concentrates purely on the division of the network into hop-zones to analytically model the approach for a large and dense network. The modeling and study of DBO aims to understand the energy and bandwidth impact of packet duplication and route convergence, not only for MERLIN but also for a whole class of directed broadcast techniques such as Directed Diffusion [Intanagonwiwat et al.

2003][Williams and Camp 2002] and address-less routing protocols [Park and Corson 1997][Braginsky and Estrin 2002][Ye et al. 2001], that can be augmented with a simple CSMA-based mechanism of packet overhearing to prune re-transmissions.

A related study by Alonso et al. [Alonso et al. 2006] considers the maximal improvement obtained through a perfect routing strategy in comparison with an ineffective routing strategy to quantify the bounds of energy consumption. Their conclusions contradict the popular belief that it is always the nodes deployed nearest to the sink that represent the bottleneck for the forwarding load and thus the network lifetime. The analysis and simulations within our work also confirm Alonso et al.'s results, illustrating that packet duplication in DBO occurs at nodes closer to the source rather than nodes closer to the sink. The study in [Krishnamachari et al. 2002] also presents a related effort on modeling general data-centric routing and comparing its performance with traditional end-to-end routing schemes in terms of energy, delay and robustness. The modeling in this paper focuses on the family of mechanisms that use directed broadcast and overhearing, rather than on generalized data-centric routing.

Most of the forwarding techniques for wireless networks and large-scale sensor networks focus on on-demand unicast techniques [Perkins and Royer 1999][Johnson and Maltz 1996], Steiner Minimal tree-based unicast such as [Lu et al. 2004], multicast and flooding techniques such as [Intanagonwiwat et al. 2000][Braginsky and Estrin 2002].

Directed Diffusion [Intanagonwiwat et al. 2003] provides a routing paradigm specifically targeted for resource constrained devices. The algorithm is data centric in that all communication is for named data. Key elements for the paradigm are: interests, data messages, gradients, and reinforcements. Directed Diffusion adopts a publish/subscribe mechanisms to obtain information from the network. Initially, a data interest from a subscriber node is propagated through the network. A node that receives an interest may then decide to forward it to its neighbours. Each node stores in its cache a database of interests following a broadcast from either the base station or a particular node. In case a publisher node matches the data interest, then a gradient between publisher and subscriber will be established. The gradient contains packet data rate and direction towards the subscriber. These parameters allow establishing different routing paths between publisher and subscriber that will subsequently be pruned through a mechanism of path reinforcement. Directed Diffusion targets applications that require node communication as peers. Furthermore, it can cope well with dynamic networks where new nodes may join or leave the network unexpectedly. However, the algorithm requires a great deal of data caching and involves gradient and path establishment, which increases packet delay and transmission overhead. In contrast, DBO optimizes node/gateway communications without requiring prior route establishment, by only storing the node hop zone.

A mechanism that resembles DBO is the Directed Flood-Routing Framework (DFRF) [Maróti 2004] which introduces a family of broadcast-based routing protocols for sensor networks. Although Maróti's paper presents only a brief description of different broadcast metrics and no quantitative analysis, it identifies the benefits of having directed broadcast over a unicast-type routing for providing higher

reliability through multiple routes. DBO builds on the DFRF framework by introducing the concept of packet overhearing *within* the same zone (which is referred to as rank in DFRF) that avoids each node re-broadcasting the same packet to reduce transmission overhead. Furthermore, the evaluation of DBO in Sections 3 and 4 shows that the multiple routes converge after a number of hops, which depends on the radio model. Finally, while the DFRF study provides qualitative guidelines on directed broadcasting and multiple routes, the DBO evaluation involves a comprehensive quantitative study that assesses the transmission overhead and the energy consumption in comparison with several flavours of greedy unicast routing.

A further related work is the ARRIVE algorithm [Polastre et al. 2003] that is based on a tree-like topology rooted at the sink of the network. The algorithm makes probabilistic decisions for packet forwarding that are based on the neighbours' states. As in DBO, ARRIVE takes advantage of the inherent broadcast nature of the medium to promote passive participation of the neighborhood. ARRIVE confirms that the usage of broadcast is effective in dealing with large patterned failures within a relatively short period of time. However, it uses unicast transmissions for the actual forwarding. This is in stark contrast with DBO that concentrates only on directed broadcasting without considering any specific forwarder. This scheme matches well also with the requirements of novel mechanisms of data aggregation such as AIDA [He et al. 2004] that may be placed at an above logical layer.

To our knowledge no work has been done to analytically model and to quantitatively evaluate the behavior of re-transmissions and route convergence for directional broadcast algorithms augmented with CSMA-based mechanism of packet overhearing/discarding, which is the scope of this work.

3. DIRECTED BROADCAST WITH OVERHEARING

DBO targets energy and bandwidth efficient data collection in sensor networks. It combines direct broadcast and overhearing for reducing control overhead of data collection. DBO differs from conventional data collection mechanisms in that it does not use beacons for exchange or maintenance of network state information. It also uses anycast transmissions rather specifying a next hop forwarder for a data packet.

The DBO design approach adopts a view that limiting the control mechanisms results in a more energy-efficient, reliable, and scalable resource management strategy in dense medium to large sensor networks. DBO is a holistic cross-layer approach that combines functionality from the routing and MAC layers, which are treated separately in conventional protocols. It builds on the three simple mechanisms of *directed broadcast*, *packet overhearing*, and *carrier sense multiple access (CSMA)*.

All nodes in DBO use **CSMA** to access the radio channel and send their packets. Following an initialization phase during which nodes progressively learn their hop count, or more generally, their cumulative path metric [UCBerkeley], from the nearest data sink, a node S that is n hops away from the gateway simply broadcasts its data packet without specifying a forwarder. The packet is received at all neighbors of node S , but only nodes that are at hop zone $n - 1$ will process this packet, while others discard it. This represents the **directed broadcast** feature

of DBO. A random node P at hop zone $n - 1$ forwards the packet to the lower hop zone. All nodes in hop zone $n - 1$ that **overhear** P 's transmission refrain from forwarding the packet and discard it, to avoid forwarding multiple copies of the same message. The process repeats at subsequent hop zones until the data sink receives the packet.

The features of DBO include:

- (1) **No Topology Maintenance:** Neither global nor local network topology state maintenance is required. The packet sender does not need to maintain any intermediate node ID, nor any specific state information about its neighbors; it merely needs to know the data sink ID and its own hop zone.
- (2) **Adaptive to Dynamic Network Conditions:** It is suitable for dynamic networks in which topology and connectivity may change rapidly and unpredictably (e.g. mobile networks). Because nodes only require their own hop zone to transmit a packet, they can adapt to topology changes whenever they overhear a changed hop zone of their neighbors. This is in contrast to data collection protocols such as MintRoute, which adapt slowly to topological changes, due to the time it takes for determining neighbors with reliable links.
- (3) **Energy and Bandwidth Efficient:** Multiple copies of a packet converge quickly toward the same path, reducing to a minimum-cost routing.

Important aspects to study are the number of duplicate packets generated by DBO in a multihop environment, the number of hops until multiple paths of the same data packet converge to a single route, and the energy consumption implications of packet duplication and route convergence. In the remainder of this section we use an idealized mathematical model to study the impact of DBO on communication overhead as the network size varies. The focus is on the duplicate packet overhead of DBO in order to compare it against the control overhead of conventional mechanisms. In addition, the analytical model investigates how quickly the multiple paths resulting from packet duplication converge to the ideal case of a single path from the packet source to the data sink. In Section 4, we implement the model to simulate the behavior of DBO packet duplication, route convergence, and energy consumption and to compare the energy consumption against several unicast routing techniques.

The remainder of this section is structured as follows. Section 3.1 presents the analytical model, followed by a sample scenario in Section 3.2 that demonstrates the route convergence in DBO. Section 3.3 concludes the analytical discussion with a mathematical justification for route convergence.

3.1 Analytical Model

While sensor networks are tightly coupled to physical environments and thus they are by definition irregular, understanding the network interactions for regular cases provides valuable insight on the trends that characterize node behavior in real networks. As a result, our model builds on assumptions that facilitate mathematical analysis and system understanding. The model assumptions are as follows:

- Single data sink:** All nodes send their packets in a multi-hop fashion towards a single data sink, denoted as D .

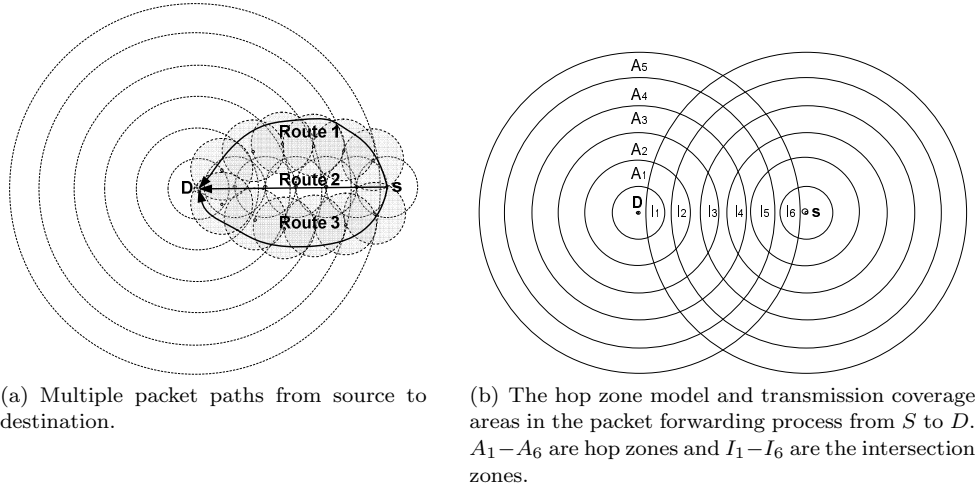


Fig. 1. Hop zone structure

- **Dense network:** The model considers a high node density, where the ratio of the transmission radius to the average internode distance is high.
- **Uniform transmission radius:** For the purposes of communication modeling, nodes are represented as points in a 2D cartesian coordinate system while each node's transmission radius is defined by a circle of transmission radius R and centered at the node itself.
- **Uniform hop zones:** Following an initialization stage, all nodes at a certain hop count i from D are assumed to be in the i^{th} hop zone, defined by the two circles centered at the destination D and with radii of $(i-1)R$ and $i * R$ [Ruzzelli et al. 2008].

Note that the simulations in Section 4 consider the effects of relaxing the ideal radio propagation assumption by incorporating non-ideal radio models and the high density assumption by considering lower node density. Section 5 further discusses the effect of relaxing all of the above assumptions on the performance of DBO.

The forwarding activity of DBO can generate multiple copies of the same packet traveling along different routes from S to D , as shown in Figure 1(a). The concentric annuli in Figure 1(a) centered at D represent the idealized hop zones, whereas the smaller overlapping circles represent the maximal transmission coverage regions of forwarders along the path from S to D . In this particular scenario, the same packet traverses three independent paths from source to destination. All packet forwarders in a particular hop zone are encompassed in the intersection region of the hop zone and the transmission coverage region of forwarders in the next higher hop zone. Our analysis approaches the problem by focusing on these intersection regions.

Figure 1(b) shows the hop zones around a destination D with the source node S located in hop zone 6. The concentric annuli A_1 - A_6 represent the hop zones and I_1 - I_6 represent the transmission coverage regions of the packet forwarders at each hop zone (the intersection regions). The model implementation includes two main stages: (1) **intersection region determination** for each hop zone along the path

from source to destination; and (2) **iterative forwarder selection** within each intersection region.

Consider a source node S , which has a packet to transmit, located at some point in hop zone n . An upstream packet transmission of S is received within a circle C_n^S centered at S with a radius R . All potential forwarding nodes of S 's packet within the annulus A_{n-1} belong to the region I_{n-1} , determined through the following expression:

$$I_{n-1} = C_n^S \cap A_{n-1} \quad (1)$$

Potential forwarders in region I_{n-1} will compete to forward the packet resulting in M_{n-1} re-transmissions to the annulus A_{n-2} . **A node transmits a packet only if no other nodes in region I_{n-1} within its transmission radius R transmit the same packet.** This packet overhearing mechanism limits the number of forwarding nodes in the region I_{n-1} . In particular, the distance between any pair of nodes in hop zone I_{n-1} that can forward the same packet must be greater than R . Each forwarding node P_j covers a transmission circle $C_{n-1}^{P_j}$ that intersects the lower annulus A_{n-2} in at least one point ². The union of such intersections yields the region I_{n-2} , defined by the following expression:

$$I_{n-2} = \left(\bigcup_{j=1}^{M_{n-1}} C_{n-1}^{(P_j)} \right) \cap A_{n-2} \quad (2)$$

where the next potential forwarders are located in region I_{n-2} . The process of forwarding a packet from S in the n^{th} annulus to D can be characterized by the set of regions $I_{n-1}, I_{n-2}, \dots, I_1$, where the following expression determines the region I_{n-k} :

$$I_{n-k} = \left(\bigcup_{j=1}^{M_{n-k+1}} C_{n-k+1}^{(P_j)} \right) \cap A_{n-k} \quad (3)$$

where $C_{n-k+1}^{(P_j)}$ represents the transmission coverage region of node P_j in annulus $n - k + 1$. In a plane densely populated with nodes, the number of forwarding nodes of the $(n - k)^{\text{th}}$ annulus correlates positively to the area of the region I_{n-k} . A larger area of I_{n-k} may cause an increase in the number of potential forwarders that are mutually separated by a distance of at least R .

It is worth noting the impact of the position of the source node and forwarders on the size (in both horizontal and vertical dimensions) of the coverage regions. A source or forwarder located at the inner edge of annulus n yields a relatively large region I_{n-1} . Similarly, a source or forwarder near the outer edge of annulus n

²The distance between the inner and the outer radius of an annulus is equal to the node transmission radius. This ensures that a transmission can always reach the lower annulus. The same is achieved in real scenarios where a node places itself in hop zone n only if it receives and acknowledges correctly from and to zone $n-1$.

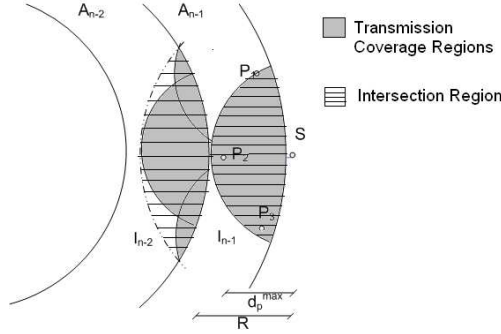


Fig. 2. Transmission coverage regions and intersection regions.

yields a relatively small I_{n-1} . This effect can be used to simplify the computation of Equation 3.

We define $d_P \in [0, R]$ as the distance of a transmitting node P from the outer edge of its annulus $n-k$. The forwarding node with the largest d_P within a region I_{n-k} determines the deepest point in region I_{n-k-1} . In particular, all points that hear transmissions from region I_{n-k} will have a distance less than or equal to d_P from the outer edge of annulus A_{n-k-1} , since the distance between annuli edges is R .

To reduce the complexity of computing I_{n-k} at each stage in the process, I_{n-k} is conservatively estimated as the intersection of the outer edge of annulus A_{n-k} and a circle that is centered at the source S , and with a radius equal to:

$$r_{n-k} = (k-1)R + d_{n-k+1}^{max}, \quad k = 1, 2, \dots, n \quad (4)$$

where d_{n-k+1}^{max} represents the largest d_P of all forwarding nodes in region I_{n-k+1} . For notational simplicity, we rename d_{n-k+1}^{max} from Equation 4 as α_k , which is further described below in Section 3.3.1.

Figure 2 illustrates the estimation of the intersection regions I_{n-1} and I_{n-2} , according to equation 4. Note that the intersection region I_{n-1} in Figure 2 coincides with C_n^S , while intersection region I_{n-2} is an envelope that encompasses the coverage regions of P_1 , P_2 , and P_3 in annulus A_{n-2} . This estimation limits the model's computational complexity, and it represents a conservative estimate of the area of all regions I_{n-k} .

Equation 4 provides the basis for modeling the data forwarding process. The model uses a two-dimensional cartesian coordinate system centered at the destination D and considers a source node S located at a distance d_S from the outer edge of annulus n . Through Equation 1, the model can determine region I_{n-1} . A random node P_1 within region I_{n-1} is selected as the first packet forwarder. In our analytical model, nodes within a neighborhood that receive a packet destined to the gateway compete to forward this packet. This occurs in a distributed manner where a random node obtains the radio channel through the carrier sense multiple access (CSMA) technique, which is employed by the non-beacon-enabled mode of the current IEEE 802.15.4 [802.15.4 2003] sensor network radio transceivers, such as Chipcon CC2420 [Chipcon 2005]. Whenever a node A receives a packet, it com-

ForEach: k=1 to n-1	Region
Determine I_{n-k}	Determination
$Q_{n-k} = I_{n-k}$	Forwarder
$j = 0$	Selection
While $Q_{n-k} \neq \phi$	
$j = j + 1$	
Select random point $P_j \in Q_{n-k}$	
Determine region $COV_{n-k}^j = C_{n-k}^{P_j} \cap I_{n-k}$	
$Q_{n-k} = Q_{n-k} - COV_{n-k}^j$	

Fig. 3. DBO Pseudocode

petes for the channel through IEEE 802.15.4's channel access mechanism (based on binary exponential backoff). If node A obtains the channel, A is designated as a forwarder P_1 and it attempts to forward the packet to the next zone. If P_1 successfully obtains the channel, it forwards the packet and sends a burst ACK message back to the sender. Any neighbor of node P_1 that overhears the forwarded packet or the burst ACK refrains from forwarding the packet. Once the sender receives a burst ACK from at least one node in region I_{n-1} , it relinquishes responsibility of the packet. At this time, node P_1 is responsible for ensuring that the packet continues moving towards the data sink. This hop-by-hop acknowledgement mechanism ensures that packets eventually reach the data sink.

Because all nodes within P_1 's transmission radius refrain from forwarding the packet, the next forwarder P_2 within I_{n-1} is another random node that is not within P_1 's transmission radius. The process of selecting a random forwarder from the yet uncovered area in region I_{n-1} repeats until all points in this region are covered by the transmission of at least one forwarder from region I_{n-k+1} . Subsequently, the model determines the envelopes of region I_{n-2} , I_{n-3} , I_{n-k} , ... I_1 through Equation 4 and proceeds to select random forwarders in each region, ensuring that all points in each region are covered by at least one packet transmission. Upon completion, the model will have determined the location and number of forwarders of the data packet in each region, enabling packet overhead and energy consumption analysis. Figure 3 summarizes the steps involved in this algorithm.

3.2 A Sample Scenario

Figure 4 shows a packet forwarding scenario that exemplifies the DBO in action. The packet sender S is located in annulus 10, with d_S equal to $0.99R$. The region I_9 containing potential forwarders in annulus A_9 is the intersection of C_{10}^S and A_9 , and is determined through Equation 1. The algorithm begins by selecting a random point P_1 within the region I_9 as a forwarder in region 9, signified by the dark ring in Figure 4(a). The lightly shaded area in Figure 4(a) represents all points in I_9 that hear P_1 's transmission and refrain from forwarding the packet.

The remaining region within I_9 that is not covered by P_1 's transmission is indicated with the dark shaded area. Because the model deals with dense networks, it is likely that a node P_2 within the dark region will also receive and forward the data packet originating at S . P_2 's transmission results in the total coverage of region I_9 , as shown in Figure 4(b). Having determined all forwarders in A_9 , the model determines the region I_8 through Equation 4.

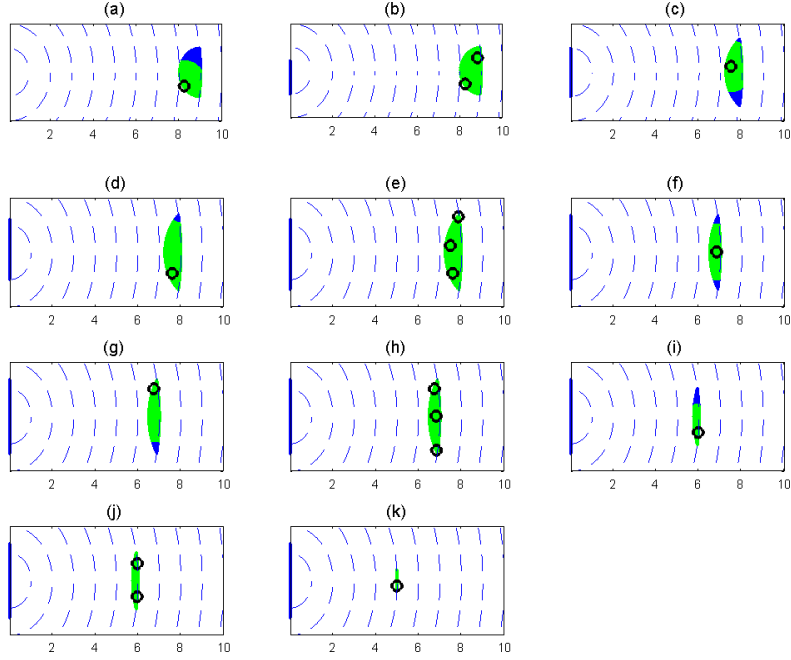


Fig. 4. A sample transmission scenario: The sender is located in annulus 10, and convergence occurs after 5 hops of relaying at annulus 5.

The forwarded packets from I_9 arrive at region I_8 , shown in Figure 4(c). Note that the region I_8 is narrower and longer than I_9 , requiring three random forwarders to cover all of I_8 (Figure 4(c)-(e)). A similar forwarding process is repeated in hop zones 8,7,6, and 5, at which point the number of forwarders converges to only one node. Section 3.3 discusses the analytical reasoning behind the apparent route convergence trend, mainly due to the shape and surface area of the regions I_{n-k} .

3.3 Convergence Analysis

The scenario in Figure 4 illustrates the convergence of packet transmissions to one packet per hop after 5 hops. In this section, we provide the mathematical justification for the convergence of packet transmissions for DBO.

3.3.1 Penetration Factor. The α_k variable represents the **penetration factor** of a packet transmission into annulus $n - k$. Clearly, α_k is always within the range $[0, R]$.

Suppose a source that is located at d_S in annulus A_n broadcasts a data packet with a transmission radius R . The penetration factor α_1 at annulus $n - 1$ is equal to d_S . Recall that the packet forwarders in region I_{n-1} are random points in this region. Thus, the distances d_P for all forwarders in region I_{n-1} are random variables in the range $[0, \alpha_1]$. Since α_2 is simply equal to $d_{P_{n-1}}^{max}$, then $\alpha_2 \in [0, \alpha_1]$. Similarly, $\alpha_3 \in [0, \alpha_2]$. Generalizing this relationship to subsequent hops in the forwarding process yields the following relationship:

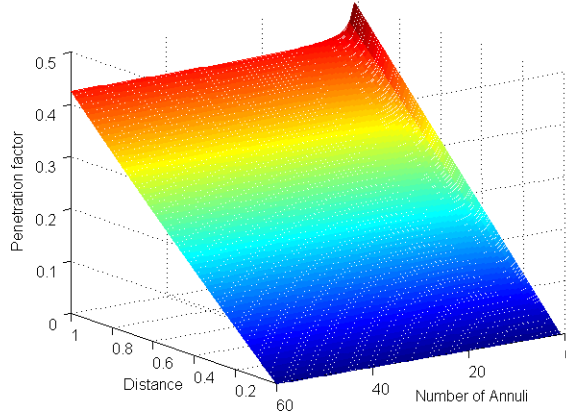


Fig. 5. The average penetration factor at annulus A_{n-1} .

$$\alpha_k \in [0, \alpha_{k-1}] \quad (5)$$

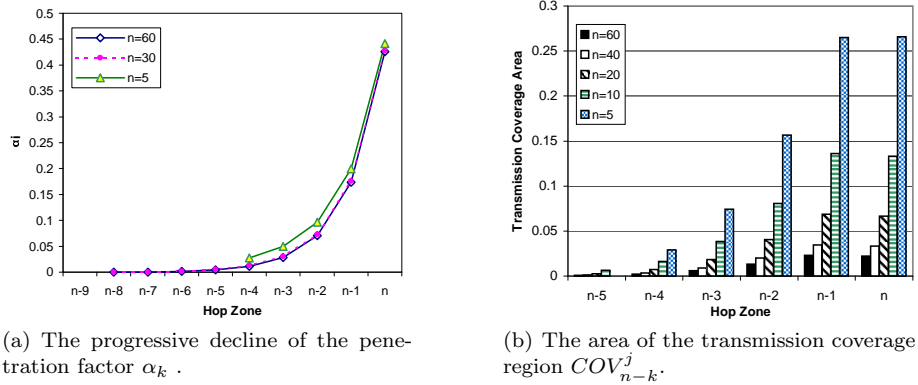
Equation 5 states that the penetration factor at every annulus is a positive random variable that is less than the penetration factor in the next higher annulus. This indicates that the transmission coverage area progressively shrinks along subsequent hops from source to destination. Route convergence occurs when the transmission coverage area shrinkage results in only one node forwarding the packet at each annulus until the packet reaches the destination.

The rate of degradation in the penetration factor series determines the rate of shrinkage of the transmission coverage area in the next annulus, and it ultimately determines the rate of route convergence for packet transmissions. In order to quantify how quickly transmissions converge in the average case, we consider that every point in region I_{n-k} has equal probability of forwarding a data packet. Thus, the point at the center of gravity of the region I_{n-k} , i.e. the centroid, represents the average case for the penetration factor since it divides the region into two regions of equal areas. Section A.1 in the appendix outlines our analytical approach for determining the centroid mathematically prior to applying the mathematical solution to the DBO model.

3.3.2 Route Convergence. How fast the packet transmissions converge to the ideal case of a single path within DBO depends on the relative size of the two intersecting circles, as indicated in the analysis in the appendix. The results there conclude that penetration factors are smaller for sources located at higher hop zones.

To validate these claims, we integrate Equation 8 from the analysis in the appendix into a process in Matlab that determines the centroid location of the intersection region between the two circles, the corresponding average penetration factor, and the coverage area for all zones in a given network scenario.

Figure 5 illustrates the penetration factor at hop zone $n - 1$ for n between 1 and 60, and for d_S ranging between 0.001 to 0.999. The figure essentially shows how deep the first packet transmission from a source at hop zone n with a distance



(a) The progressive decline of the penetration factor α_k .

(b) The area of the transmission coverage region COV_{n-k}^j .

Fig. 6. The penetration factor and coverage region

d_S will penetrate into zone $n - 1$. The effect of distance is clearly apparent from the plot, as sources with a smaller d_S always have a smaller penetration factor into hop zone $n - 1$. In the worst case scenario for d_S close to R , the penetration factor at zone $n - 1$ for large networks is just above $0.4R$. The penetration factor is noticeably higher for smaller networks with n less than 7 hops.

Figure 6(a) plots the penetration factor of the centroid α_k versus the hop zone number for values of n equal to 5, 30, and 60, and for d_S equal to 0.999, representing the worst case scenario when the source is at the edge of the lower hop zone. For simplicity and without loss of generality, the value of R is set to 1. The penetration factor for all three plots converges to zero after 5 hops, indicating that packet duplication occurs mainly in the first 5 hops from the source. The three plots also follow a similar trend, with slightly larger penetration factors for $n = 5$. Larger penetration factors for sources within fewer hops away from the destination stem from the smaller ratio of F to r_{n-k} for these sources, as discussed above.

Figure 6(b) illustrates the transmission coverage area as packets traverse the network for the source towards the destination, again assuming that α_k is defined by the centroid of region I_{n-k} . The transmission coverage area is much higher for sources with smaller n , although the penetration factors from Figure 6(a) do not exhibit large differences. The transmission coverage area converges towards zero after 5 hops, which is in line with the results of Figure 6(a)³. Section A.2 in the Appendix elaborates further on this effect.

In sum, the analytical results indicate that in a dense network where nodes are randomly distributed, the transmission coverage area is always larger for packets sourced closer to the destination. The large transmission coverage area for sources with smaller value of n increases the probability of multiple packet transmissions at next lower hop zones. The average number of hops for the transmission coverage area to become sufficiently small so that a single node forwards the data packet is five hops for all considered source locations, confirming the quick convergence of transient multiple paths to a single path.

³Note that for Figure 6(a), the plot for $n = 5$ ends at hop $n - 4$, as the packet reaches the destination at that point.

4. MODEL IMPLEMENTATION AND SIMULATIONS

In order to identify the benefits of the DBO approach, we develop a Matlab process that models its behavior. The aim of implementing the DBO in Matlab is to accurately model the sequence of packet transmissions and the resulting energy consumption for a multi-hop network. The model uses a two-dimensional cartesian coordinate system with the data sink D located at $(0,0)$ and the source node in hop zone n located at $(nR - d_S, 0)$. The minimum separation unit between any two points in the model is $0.01R$, providing sufficient granularity for modeling high density networks. As in Section 3, the value of R is set to one.

The model runs the pseudocode in Figure 3 and stores the value of the variable j for each hop zone, which indicates the per zone packet transmissions as the packet is relayed from source to destination. The model also stores the coordinates of all forwarders P_j for later analysis.

To quantify the effect of d_S on the packet forwarding overhead, the simulations consider six different values for d_S : 0.01, 0.2, 0.4, 0.6, 0.8, and 0.99. Note that 0.01 represents the best case where the source is near the outer edge of the zone, and its transmission barely penetrates into hop zone $n - 1$. The worst case is represented by $d_S = 0.99$ where the source is at the border with the inner boundary of the zone, so the source transmission has maximum penetration into hop zone $n - 1$. Six values for n are also considered to evaluate the effect of network size on packet forwarding activity: 10, 20, 30, 40, 50, and 60. For each scenario characterized by a pair of values for n and d_S , the simulation is run 10 times to obtain results that are unaffected by specific conditions that may arise in a particular simulation run. All the figures below show the average results over the 10 runs.

The remainder of this section is structured as follows. Section 4.1 investigates the effect of source hop zone and position on packet duplication. Section 4.2 further explores packet duplication and route convergence under three radio models, whereas Section 4.3 extends the model for measuring energy consumption of DBO.

4.1 Source Zone and Position

The first set of simulation results summarizes the joint effects of the source hop count n and the source position d_S within its hop zone on packet transmission overhead. Figure 7 plots the number of packet transmissions, where each of the six plots corresponds to a different source hop count n . The distance axis within each plot indicates d_S for a particular packet count, and the annulus index indicates the hop zone. In the ideal case, one packet is forwarded at each annulus so a packet sent from zone n requires n transmissions. All the plots in Figure 7 converge to the ideal case of a single packet transmission per zone after a limited number of duplicate transmissions.

The dependance of packet duplication on d_S is apparent in all the plots, as the forwarding of packets originating from nodes with a small d_S quickly converges to a single packet transmission per zone. This is attributed to the fact that a source node with a lower d_S covers a smaller area in A_{n-1} , resulting in a smaller penetration factor α_1 and in quicker convergence of subsequent penetration factors towards zero. Similarly, distances d_S with values close to one cause higher penetration factors at subsequent zones, resulting in slower convergence. *The highest duplication occurs*

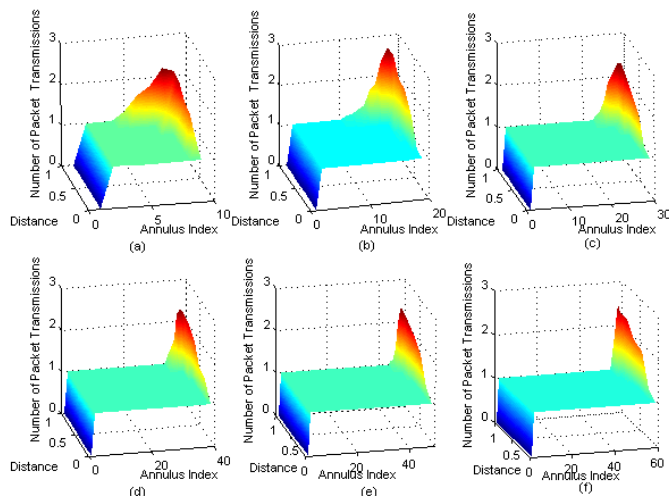


Fig. 7. The average number of packet transmissions at each annulus based on the location of the source node within the outer annulus. Six cases for the source hop count from the data sink are considered (a) 10 hops (b) 20 hops (c) 30 hops (d) 40 hops (e) 50 hops (f) 60 hops.

when d_S is 0.99, where two to three copies of the packet are generated in the first few hops before converging again to the ideal case of one packet transmission per zone. Note that the duplication effect is greatly reduced for values of d_S of 0.6 or lower, indicating a high probability of much quicker convergence.

4.2 Packet Duplication and Convergence

As the worst case occurs for d_S equal to 0.99, we fixed d_S to this value and ran a second set of simulations for n ranging from 10 to 60 zones, with an increment of 10, with 10 runs for each scenario. The experiments consider three different radio models by varying the grey region width. The first model considers that all nodes within a sender's transmission range receive a packet with probability one. We refer to this model as the ideal reception model ($R=1$). The second model considers that all nodes within $0.66R$ of the sender receive its transmission with probability 1, whereas nodes that are between $0.67R$ and R are in the sender's grey region. The probability that nodes in the grey region receive the packet is distributed according to a uniform random variable with a mean of 0.5, as suggested in the recent study by Srinivasan et al. [Srinivasan et al. 2006]. We refer to this model as the narrow grey region model. The third radio model considers a perfect reception region with $0.33R$ of the sender, while nodes that are between $0.34R$ and R are in the grey region and they receive the sender's packet with a uniform random probability between 0 and 1. We refer to this model as the wide grey region model.

Figure 8 shows the average number of hops for route convergence of transmissions to the ideal one packet per hop zone, with the error bars indicating the 95% confidence intervals. For the ideal reception radio model, the average number of hops till route convergence is about 5 hops for sources located at hop zone 30 or higher, confirming the analytical results in Section 3. Although the average hops till convergence for sources at zones 20 and 10 vary slightly, their corresponding

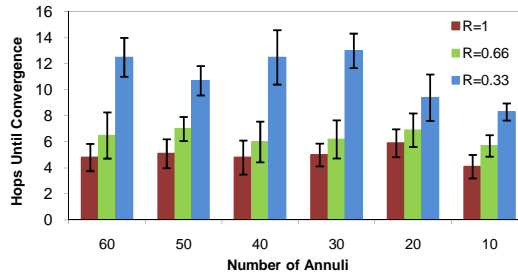


Fig. 8. The average number of hops required for convergence, as the source zone n varies. The error bars show the 95% confidence intervals.

95% confidence intervals indicate that route convergence also takes between 3 and 7 hops. For the narrow grey region model, the mean hops till convergence is around 7 hops, with an apparent independence of the hop zone of the source node. The 95% confidence intervals indicate that the average hops till convergence can vary between 4 and 8 hops. These results imply that intermittent connectivity among nodes that are located within the outer third of the source's communication range only causes an increase of 2 hops till convergence, on average, over the ideal reception model. In contrast, the wide grey region model exhibits a significant increase in hops till convergence to 10-13 hops for sources at zone 30 or higher, and 8-9 hops for sources closer to the base station.

The results in Figure 8 indicate that packet duplications occur close to the source node. In the ideal reception model, packet duplication only affects nodes that are three to seven hops away from the source. Intermittent connectivity and packet losses for narrow grey regions causes packet duplication to affect nodes within six to eight hops from the source, while a wide grey region results in packet duplication at nodes that are up to 12 hops away from the source. Packet duplication at nodes that are relatively close to the source implies that, in large networks, packet duplication does not affect nodes near the sink. This is a favorable property of DBO since the lifetime of sensor networks usually depends on the energy consumption of nodes that are near the data sink (critical nodes), which consume more power for forwarding packets arriving from nodes further away [Jurdak et al. 2007]. Because packet duplication occurs only within a few hops of the source, critical nodes are not affected by this duplication for sources with n higher than ten. In fact, packet duplication in DBO at zones that are distant from the destination only uses reserve energy at nodes close to the source that would have been unused anyway once the critical nodes die and the network loses connectivity. As a result, DBO provides a form of energy balancing between critical nodes, which tend to have a higher forwarding load, and nodes near the source, which have an increased probability of forwarding due to packet duplication. Section 4.3 discusses the energy implications of packet duplication and radio models further, including the interplay between quick route convergence and energy efficiency.

Figure 9 shows the average packet transmissions per zone for the second simulation set with $d_S = 0.99$ for each of the three radio propagation models. For each radio model, the plots for all network sizes follow mostly the same pattern. A brief

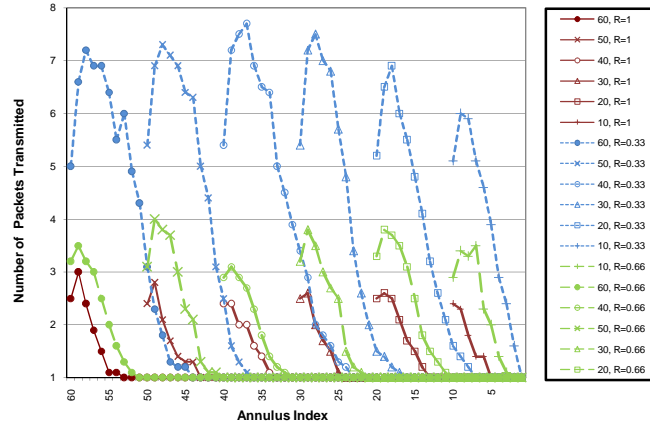


Fig. 9. Packet transmissions at each annulus for the worst case of the source located at the edge of the inner annulus. The six plots show six scenarios of source hop count from the data sink.

initial rise in packets per zone is caused by an elongation of region I_{n-1} . This rise is then offset by the effect of the shrinking penetration factor (see Section 3.2), which causes the width of the I_{n-k} to decrease. The number of average packet transmissions then continues to fall steadily for a few hops, until it finally converges to the optimal single packet transmission per zone.

The narrow grey region model exhibits a slight increase in packet duplication over ideal reception, ranging between 0.5 and 1.5 more packets at the first few hops after the source. Note the highest number of packet duplicates for narrow grey regions is 4, for nodes at zone 48 forwarding a packet originating at zone 50. The packet duplicates also take more hops to converge with narrow grey regions. The reason for the increased packet duplication is that some nodes in the grey region that have heard the original packet from the source do not hear the forwarding of that packet by one of their neighbors. As a result, one or more of these nodes also forwards the source node's packet, resulting in higher duplication.

For wide grey regions, we note a large increase in packet duplication for all network sizes. This starts with about 5 duplicates at zone $n-1$, surges to over 7 duplicates at $n-3$, before decreasing steadily and converging after 8-12 hops. The increased duplication for the wide grey region model is simply because of the more pronounced effect of packet losses, which causes more nodes in the grey region to forward the same packet due to their failure to overhear other forwarded packets in their neighborhood.

Figure 10(a) plots the total number of packet transmissions for a packet sent from hop zone n to reach the data sink for $d_S = 0.99$. The 3 bar graphs correspond to the three radio models under consideration. The horizontal axis indicates the values of n , which range between 10 and 60 hop zones. Recall that the ideal number of packet transmissions for a source located n hops away from the data sink is equal to n . The results in Figure 10(a) show that, for ideal reception, the average number of transmissions for a packet to reach the data sink from a source at zone n is between $n + 4$ to $n + 7$ packets. For narrow grey regions, the average transmissions

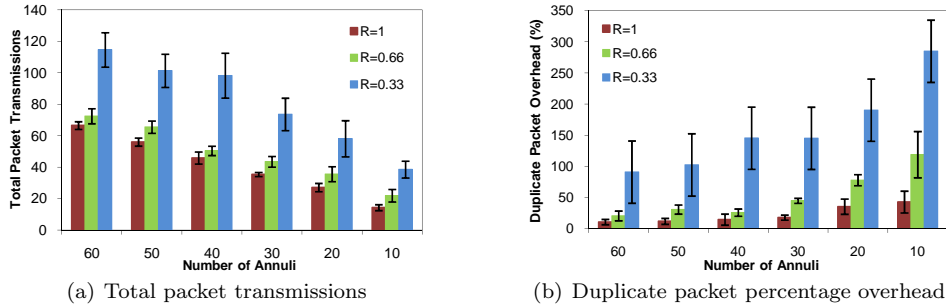


Fig. 10. Packet duplication with DBO for $d_S = 0.99$ and a network radius ranging from 10 to 60 hops. The error bars show the 95% confidence intervals.

for a packet to reach the sink range between $n + 11$ to $n + 15$ packets. Finally, a wide grey region causes significant increases in total packet transmission that vary widely based on network size.

To put the packet transmission results in perspective, Figure 10(b) plots the overhead of the duplicate packets for all three radio models as a percentage of the ideal number of packet transmissions for a source located in zone n . The results clearly indicate that the percentage overhead is lower for large networks, while it grows significantly for smaller networks. Recall from Figure 10(a) that the number of packet duplicates for DBO is almost the same for a given radio model regardless of network size. However, the same duplicate packet count represents a much larger percentage overhead for small networks, where the ideal case involves a small number of packet transmission. For example, large networks, such as the case of 60 zones, inherently involve a large number of packet transmissions for relaying a packet from source to destination, so the duplicate packet overhead of 4 to 7 packets in the ideal reception model case or 11 to 15 packets for narrow grey regions represents a 10% to 20% overhead of packets respectively. In contrast, the overhead in smaller networks of ranges between 43% and 285%, depending on the radio model. This suggests that DBO is better suited for larger networks.

The results in this subsection have revealed two properties of DBO: (1) packet duplication occurs mainly near the source node, whereas route convergence occurs after a few hops; (2) the applicable radio model, which captures the effects of packet losses and intermittent connectivity, plays a major role in determining the extent of packet duplication and how quickly the multiple routes converge. The next subsection explores the implications of these properties on energy consumption.

4.3 Energy Consumption

We have modeled energy consumption in sensor networks in order to evaluate the benefits of DBO. We consider the current draw and power consumption values of the CC2420 radio [Chipcon 2005]. The power consumption P_t of CC2420 in transmit mode is 52.2 mW, while its power consumption in receive mode P_r and listening mode is 59.1 mW. The simulation model tracks the time each nodes spends transmitting packets, receiving packets, listening to the channel, or sleeping. The time spent in each radio state along with the power rating in that state enables the

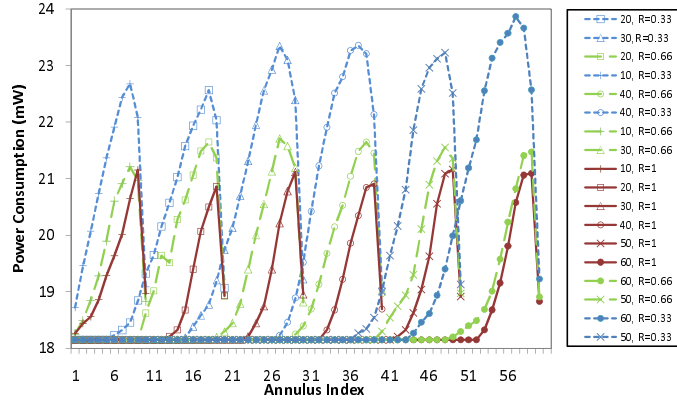


Fig. 11. Average power consumption P at each hop zone during the forwarding of a packet from hop zone N to the base station. The results include 3 radio models that vary the width of the grey region around the source. Note that the power axis does not start at zero to highlight the relative differences for the 3 radio models.

model to determine the total energy consumption of each node by summing up all the components for each node:

$$E = P_t \times T_t + P_r \times T_r + P_l \times T_l + P_s \times T_s \quad (6)$$

where T_t is time spent in transmit mode, T_r is the time in receive mode, P_l and T_l are the power and time for listening mode, and P_s and T_s are the power and time for sleeping mode respectively. The average power consumption of each nodes is then computed through the following expression:

$$P = E/T \quad (7)$$

where T is the total duration of a deployment (or simulation).

In DBO, nodes are in receive mode when they overhear transmissions in their vicinity, whether these transmissions are original data packets, forwarded data packets, or burst acknowledgements. Nodes only go into transmit mode to send or forward a packet, or to send a burst acknowledgement. Nodes spend the remainder of their awake time in listening mode to check the channel for activity, yielding T_l . The sleeping time T_s is simply the difference of the total simulation time T and T_t , T_r , and T_l . All the simulations for evaluating energy consumption conservatively consider the worst case source position at $d_S = 0.99$. The model considers a radio duty cycle of 30% for all nodes.

Figure 11 plots the average power consumption per node at each annulus resulting from the packet duplication scenarios in Figure 9. The power consumption follows a similar trend to packet duplication, with higher power consumption at zones with more duplicates. These nodes are always located in the zones close to the source node. As for nodes further away from the source, the power consumption remains low and constant as a result of quick route convergence.

A notable feature of the energy consumption plots is that the impact of packet duplication on power consumption is limited. For example, a transmission generates an average of 3.5 duplicates at zone 60 for narrow grey regions, and the same

transmission generates 2.5 duplicates at zone 60 for ideal reception. However, the average node power consumption difference at zone 60 for the two cases differs by only 0.33 mW, which represents a 1.66% difference. Similar observations can be made for wide grey regions and for different network sizes. This effect stems from the dominance of the listening energy on the consumption of the nodes.

For a given radio model, the power consumption is relatively independent of the source hop zone position, except for wide grey regions, where sources further away from the base station cause an increase in power consumption per node.

We now compare the power consumption of DBO to other routing techniques. For this purpose, we consider two versions of greedy unicast routing that typify sensor network routing protocols: (1) unicast routing based on overhearing with no beaconing; (2) beacon-based unicast routing. In the first version, nodes snoop on packets from their neighbors to build up and store routing state locally. Nodes can use this routing state in selecting a routing parent. The latter version broadcasts periodic beacons locally to advertise neighborhood state, which causes an increase in T_r that depends on the neighborhood size. It considers a parameter D that quantifies the node density through neighborhood size, which directly impacts the number of beacons each node receives.

The main tradeoffs between the unicast routing techniques and DBO are as follows. DBO involves packet duplication at zones near the source, which causes nodes energy overhead at these nodes. Energy consumption due to beaconing or snooping in unicast techniques is mostly independent of the node's location in the routing tree, as it is caused by local transmissions. However, the convergence of all packets to the base station causes nodes near the base station to have a higher forwarding load than nodes at the edge of the network. This can cause incremental increases of power consumption at critical nodes near the base station, leading to a quicker energy depletion at these nodes.

Because unicast routing selects a parent for each node, a parent in the grey region may not receive a transmission, which causes the source to retransmit the packet. This represents energy overhead in unicast routing, whereas the lack of parent designation in directed broadcast avoids retransmissions. Another cause of energy consumption for beacon-based routing techniques is local broadcast of beacons, which can be avoided in directed broadcast. Our simulations consider that each node sends a beacon message every minute, and that beacons are asynchronous across nodes. The size of the beacon message is one half that of data packets.

Figure 12 plots the power consumption for DBO, beacon-less unicast routing, and beacon-based unicast routing with values of $D=5$ and $D=10$, under the ideal reception model. Figure 12(a) considers a source located at hop zone 10. In all the unicast techniques, the power consumption is independent of the annulus index. Both plots for beacon-based unicast routing exhibit significantly higher power consumption per node, as nodes must receive and process periodic beacons from their neighbors. As expected, the power consumption for $D=10$ is higher than $D=5$ because the higher density generates more beacons in a neighborhood. The power consumption for beacon-less unicast routing is significantly lower than beacon-based routing, and it is slightly lower at edge zones that overhear fewer packet retransmissions. The power consumption for DBO is slightly higher than beacon-less unicast

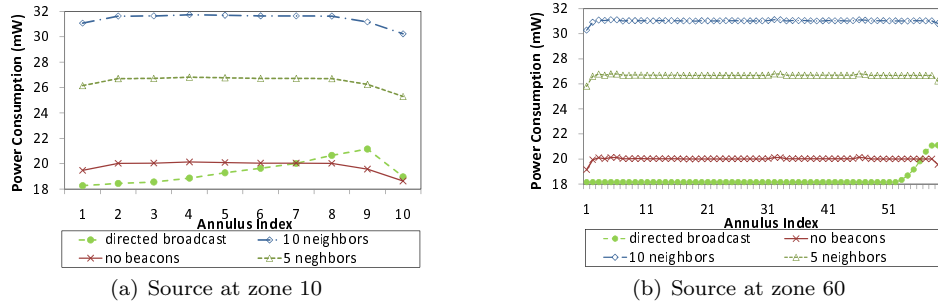


Fig. 12. Comparison of the average power consumption for directional broadcast, beaconless unicast routing, beacon-based unicast routing with $D=5$, and $D=10$, with no grey region. Note that the power axis does not start at zero to highlight the relative differences at each hop for the 4 protocols.

routing for hop zones 8-10, and it is lower for zones 1-6. In fact, visual comparison of the area between the plots of DBO and beacon-less routing indicates that DBO consumes less overall energy than beacon-less routing. In addition, the power reduction of DBO at zones closer to the base station reflects positively on network lifetime, as it is these nodes that are critical for maintaining network connectivity. The savings of DBO at zones 1-6 stem from the shrinking of the penetration factor, which causes fewer nodes to overhear transmission at every subsequent hop. In contrast, beacon-less routing, which uses a greedy approach to minimize the hop count from the source to destination, does not shrink the penetration factor, so more nodes overhear and process the packets at every hop, causing increased power consumption for beacon-less routing.

Figure 12(b) plots the average power consumption per node for the four routing techniques when a source is located at hop zone 60. The power consumption for the three unicast techniques is nearly the same as in Figure 12(a) because energy consumption in these techniques is dominated by local transmissions, including local beacon broadcasts and packet overhearing, which is independent from the hop zone. For this scenario, DBO consumes more energy than beaconless unicast up to four hops away from the source (compared to two hops for Figure 12(a)). However, the power consumption for DBO is about 15% lower than beaconless unicast routing for all other hop zones, as a result of greedy forwarding in the latter which causes more nodes to overhear packets. The energy savings for DBO at zones 1-55 significantly outweigh its energy overhead at zones 56-60, especially since its packet duplication does not affect critical nodes near the base station.

Figure 13 shows the results for the same scenarios with narrow grey regions. Again, DBO consumes significantly lower energy than beacon-enabled routing for both sources at zone 10 and 60. The power consumption for beacon-enabled routing with $D=10$ does however decrease slightly because the grey regions cause nodes to overhear fewer beacons on average in their neighborhood of 10 nodes. The same effect can be seen for $D=5$, but it is less pronounced as the reduction in beacon overhead is proportional to neighborhood size. Note the minor fluctuations of the power consumption among nodes at different hops for the unicast routing due to variable numbers of retransmissions at every hop when the parent node fails to

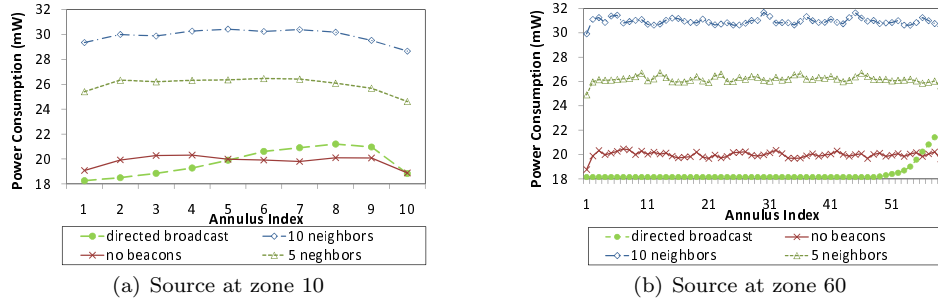


Fig. 13. Comparison of the average power consumption for directional broadcast, beaconless unicast routing, beacon-based unicast routing with $d=5$, and $d=10$, with $R=0.66$. Note that the power axis does not start at zero to highlight the relative differences at each hop for the 4 protocols.

receive the packet due to intermittent connectivity within the grey region. The plot for a source at zone 60 reveals a similar behavior to the case of ideal reception when comparing DBO and beacon-less unicast. For a source at zone 10, the cross-over point between the two plots for DBO and beaconless unicast shifts from zone 7 for ideal reception to zone 5 for narrow grey regions, indicating that only zones 1-4 benefit from using DBO. We also note that the energy savings of DBO for zones 1-4 are nearly equal to its energy overhead for zones 6-10 when comparing it with beacon-less unicast. While DBO does not seem to reduce the overall energy consumption for narrow grey regions, it does shift away the energy overhead from critical nodes to non-critical nodes, which promotes network longevity. The increased power consumption for DBO at zones 6-10 is due to the grey region, which causes some nodes that overhear the source's transmission to not overhear the forwarder's transmission, and to retransmit the packet themselves.

In addition to shifting the power consumption away from critical nodes, DBO can provide a higher degree of reliability over beacon-less unicast with intermittent connectivity and packet losses. In unicast routing, a node sends a packet to its designated parent. If the parent does not receive the packet, the node must retransmit the packet, possibly multiple times, until the parent receives it. In contrast, while some nodes may lose packets with DBO, other nodes will hear the packet, especially in a dense deployment. One of the nodes that hears the packet will forward it without any need for retransmission from the original packet source. Because of the burst hop-by-hop acknowledgements of packets, packets are guaranteed to reach the next hop zone. Otherwise, the current forwarder retransmits the packets until it receives an acknowledgement. While we expect DBO to have higher reliability than unicast routing, the quantitative verification of DBO's reliability is beyond of the scope of this paper.

Finally, Figure 14 considers the same scenarios as above for wide grey regions. For a source at zone 10, DBO exhibits a significant increase in power consumption at almost all nodes, as the effect of not overhearing neighboring forwarders is amplified with the larger grey region. For this radio model, all nodes at zones 3-10 have higher power consumption with DBO than with beaconless unicast routing. As a result, directed broadcast has a higher overall power consumption than beaconless

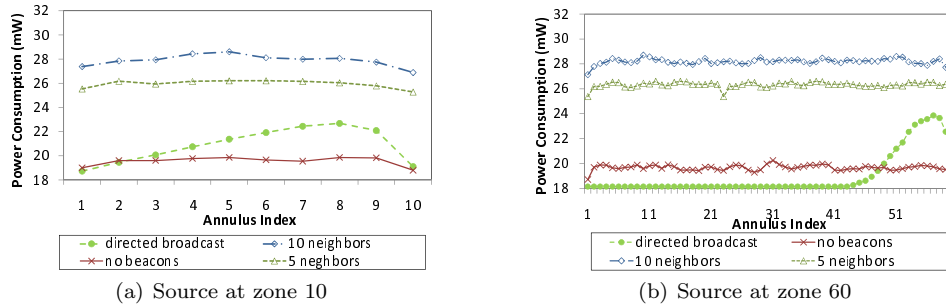


Fig. 14. Comparison of the average power consumption for directional broadcast, beaconless unicast routing, beacon-based unicast routing with $d=5$, and $d=10$, with $R=0.33$. Note that the power axis does not start at zero to highlight the relative differences at each hop for the 4 protocols.

unicast routing, with only slightly reduced power consumption with DBO at zones 1 and 2. Beacon-based routing techniques exhibit a further reduction in power consumption, as fewer nodes overhear beacons and data transmissions due to the wider grey region. In fact, the plot of $D=10$ moves closer to the plot of $D=5$ for this scenario, as nodes save more energy when they miss beacons from their denser local neighborhood. However, the reduction in power consumption beacon-based routing is truncated by the increased possibility of retransmissions between the node and its parent. DBO still consumes significantly lower energy than both versions of the beacon-based unicast routing. For a source at zone 60 (Figure 14(b)), nodes near the source consume higher energy with DBO. However, DBO still maintains its energy savings over beacon-based unicast. The difference in power consumption between DBO and beacon-less routing is larger with wide grey regions for nodes near the source. However, the energy overhead of DBO at these nodes is counterbalanced with energy savings at nodes in the 60 zone network closer to the base station.

The energy analysis of directed broadcast with overhearing in this section has revealed that packet duplication at the nodes close to the source causes these nodes to have higher power consumption than all other nodes, whereas it does not affect other nodes. power consumption also increases for a wider grey region. In comparison to beacon-based unicast routing, DBO has lower power consumption regardless of neighborhood size or radio model. In comparison with beaconless unicast routing based on snooping, DBO reduces power consumption at nodes closer to the base station and increases it at nodes closer to the source. The overall energy consumption for DBO is lower than all unicast routing techniques for large networks. As for smaller networks, for the ideal reception model, DBO has lower overall power consumption than beaconless unicast. While the overall power consumption of DBO relative to beaconless routing increases as the grey region widens, narrow grey regions yield nearly equal power consumption for both routing techniques with DBO

having the advantage of shifting energy consumption from critical nodes near the base station to other nodes near the source.

5. DISCUSSION AND CONCLUSION

Both the analysis and simulations have confirmed that DBO reduces network-wide communication overhead when the source is located more than 20 hops away from the nearest data sink. The reduction in overhead stems from the elimination of the control messaging exchanges synonymous with conventional protocols, which, when repeated along a lengthy path, create excessive load for all nodes along that path. This section explores the impact of relaxing each of the main assumptions of DBO in Section 3 separately.

5.1 Multiple Data Sinks

DBO can support multiple data sinks. Nodes can initially learn their hop zone progressively from the nearest data sink. Nodes in the immediate vicinity of a base station set their hop zone to one. Nodes in the next hop zone set their zone to two, and so on. If a node at zone n relative to a data sink B_1 discovers that it is m hops away from another base station B_2 , where $m < n$, then the node resets its zone to m and adopts B_2 as its data sink. Each node associates only with one data sink to which it has the least hop count. Nodes can indicate their associated data sink in the data packet so that other nodes only consider forwarding incoming packets that are associated with the same base station.

The simulation results of Section 4 can easily be extended to a multiple data sink scenario. Through the progressive hop zone discovery method, all nodes associate with the closest base station. At this point, each cluster of nodes associated with a particular data sink functions as an independent network during steady state operation. During deployment, some nodes may discover a closer data sink and alter cluster association, as a result of fluctuations in network conditions (such as node failure, node mobility, interference changes, etc.) which cause the logical topology to change. Such changes in association occur seamlessly with nodes locally deciding to switch data sink and including the identity of the new data sink in their data packets.

5.2 Reliability

DBO can provide a higher degree of reliability than conventional unicast routing techniques. Instead of designating a node as the receiver of each packet, DBO forwards packets to all nodes closer to the base station than the sending node. In case node battery depletion or intermittent connectivity cause some nodes to miss data packets, other nodes will still receive the packet and process it for possible forwarding. Using a unicast routing technique would require the sending node to retransmit the packet until the designated parent receives the packet. In case this parent has left the network due to mobility or battery depletion, then the node must choose a different parent and try the transmission again. Thus, we expect the redundancy in potential forwarders within DBO to provide it with higher reliability than unicast routing. An interesting direction for future work is to quantify the reliability of DBO and compare it to the reliability of current unicast routing protocols.

5.3 Lower Density

Another model assumption is high network density. Relaxing this constraint and considering lower density networks results in quicker convergence towards the ideal case. In networks with a lower density, it is likely that the number of forwarders at each hop zone decreases, causing coverage regions and penetration factors in subsequent zones to shrink more rapidly.

There is no risk that the lower node density coupled with directed broadcast with overhearing will cause network disconnection. By definition, a node classifies itself in a particular hop zone on the basis of packets it hears from nodes at the lower hop zone [Ruzzelli et al. 2008]. The node then confirms the bidirectional communication capability with nodes at lower layers by sending an acknowledgement, ensuring bidirectional communication between nodes at hop zones n and $n - 1$.

5.4 Non-Ideal Zones

The assumption of circular hop zones also represents an idealized situation. In reality, hop zones have irregular shaped rings that are concentric at the associated data sink. The actual shape of hop zones does however resemble circular rings that grow in size for nodes that are further away from the data sink. Although concavities and convexities in the shapes of the hop zones may occur, these do not affect the overall convergence trend for DBO. Results from the circular annuli can be generalized with confidence to the average behavior of real irregular hop zones, as confirmed in the discussion in [Ruzzelli et al. 2008].

5.5 Energy Balancing

The results in Section 4 show that most of the packet overhead for DBO occurs at nodes within few hops from the source node. For large networks, packet duplication occurs at nodes that are far away from the data sink, while critical nodes are unaffected. Critical nodes that are close to the base station are already responsible for forwarding a relatively large number of packets converging from nodes that are further away [Jurdak et al. 2007], and they typically consume energy at a higher rate than other nodes, causing them to deplete their battery resources sooner. The battery lifetime of sensor networks thus depends on the energy consumption rate of these critical nodes. The transient packet duplication of DBO at the first few hop zones has little or no effect on network lifetime for networks with large n . As a result, packet duplication in DBO represents a form of energy load balancing. This is especially useful in sensor networks that rely on solar power for their operation. Each day, nodes harvest a bounded amount of energy. Maintaining the connectivity of these networks depends on limiting the energy consumption of all nodes, particularly critical nodes, to their available daily energy. Again, the packet duplication overhead of DBO at nodes far away from the sink only means that these nodes consume a larger portion of their available daily energy.

5.6 Unfavorable Physical Topology

There are extreme physical topologies in which the DBO approach does not lead to route convergence. For instance, consider the case where a sender and data sink are located at opposite ends of two hallways. Each hallway encompasses a dense

deployment of sensor nodes, but signals transmitted in one hallway do not reach the other hallway due to attenuation in the walls. When the sender transmits a packet, nodes in each hallway forward the packet. The overhearing mechanism in DBO has no effect for transmissions through the walls, so two copies of the packet traverse the network, with one copy in each hallway, until they reach the sink at the other end. If the number of hops between the sender and the data sink is more than 5 in each hallway, DBO leads to route convergence within each hallway but not on a global network scale. This example represents an unfavorable physical topology that prevents global route convergence with DBO. For this particular example, the use of address-based routing would avoid packet duplication. However, the example above represents a very specific and highly unfavorable physical topology, while it is safe to assume that DBO generally does achieve route convergence in random topologies.

5.7 MAC Backoff Interval

In DBO, nodes that receive a packet attempt to forward it after a random MAC backoff time. Our model and simulations implement a static random transmission interval that is chosen according to the IEEE 802.15.4 specifications. However, tweaking the backoff interval may have an impact on the performance of DBO. For instance, a large interval may result in a long transmission delay while it has the advantage of reducing packet collisions within the same neighborhood. This trade-off well reflects the CSMA period of a real system in which nodes select a random time and listen to the channel for a clear channel assessment (CCA) period before transmitting. CSMA is used by WSN radios to avoid collisions due to concurrent transmissions with the neighbouring nodes. Modeling the length of the CSMA period is beyond the scope of this paper; however, an algorithm that optimizes the length of the period according to neighbouring size and end-to-end latency dictated by the application is indeed an interesting future work.

5.8 Broadcast Cost of Low-Power MAC Protocols

Previous work on low power MAC protocols for sensor networks has shown that broadcast transmissions are significantly more expensive than unicast transmissions. This effect arises mainly from the overhearing problem, where nodes that are not intended receivers of a transmission keep their radios active, which is a waste of energy. The DBO energy model actually includes the impact of overhearing, and all the power related results account for this energy overhead. Despite this inherent cause of energy overhead, DBO still outperforms beaconing protocols, while snooping protocols have the same overhead as DBO as they snoop on all packets in the neighborhood.

In sum, this paper has presented a directed broadcast with overhearing approach (DBO) for efficient resource management in sensor networks. While conventional WSN approaches rely on the introduction of control mechanisms for efficiently managing energy and bandwidth, DBO takes a step in the opposite direction by providing only basic communication functionality to the node combining CSMA,

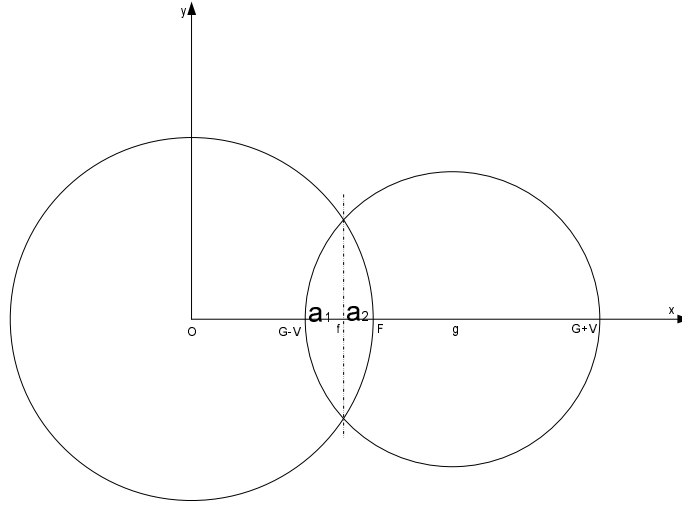


Fig. 15. Estimating the centroid of the intersection region of the current hop zone and the transmission coverage region.

packet overhearing, and directed broadcast. Analytical modeling and simulations have confirmed that the packet duplication overhead of DBO shrinks as the network size grows, rendering it more energy-efficient for large and dense sensor networks.

APPENDIX

A.1 The Centroid

We wish to find the centroid of the area formed by the intersection of two circles, as shown in Figure 15. One of the circles is the outer boundary of the current annulus and the other circle is the coverage region of transmissions originating in the higher annulus. The centroid is the center of mass of the region i.e. the point at which the region would balance on a nail, and it represents the average case for penetration of transmissions into lower zones. While the analysis in this section models DBO transmissions in any hop zone, the appendix provides a detailed analysis of the upper bounds on the number of forwarders in the first hop zone $n - 1$.

We take the first circle centered at $(0, 0)$ and with radius F , characterized by the equation:

$$x^2 + y^2 = F^2$$

and the second to have center $(g, 0)$ and radius V with equation

$$(x - g)^2 + y^2 = V^2,$$

Assuming these intersect we may easily solve the two equations to find the only x -coordinate of their point(s) of intersection:

$$(x - g)^2 + (F^2 - x^2) = V^2,$$

so

$$x = \frac{F^2 + g^2 - V^2}{2g},$$

and we set f to be equal to this value. We now consider the chord of the first circle bounded by $x^2 + y^2 = F^2$ and $x = f$. This chord has area

$$a_1 = 2 \int_f^F \sqrt{F^2 - x^2} dx$$

$$a_1 = \frac{\pi F^2}{2} - f\sqrt{F^2 - f^2} - F^2 \sin^{-1} \frac{f}{F}.$$

Taking $f = 0$ yields the area of the semicircle equal to $\pi F^2/2$. We now consider the chord to be a plate of uniform density 1, so that its mass will be a_1 . We next find the first moment of the chord about the y -axis

$$M_1 = 2 \int_f^F x\sqrt{F^2 - x^2} dx.$$

We set $w = F^2 - x^2$, so $dw = -2x dx$. The integral becomes

$$\int_0^{F^2-f^2} w^{1/2} dw = \frac{2}{3} [w^{3/2}]_0^{F^2-f^2} = \frac{2}{3} (F^2 - f^2)^{3/2}.$$

By symmetry the y -coordinate of the centroid of this chord, the other one and indeed the whole region is 0. Now the x -coordinate of the centroid of the first chord is

$$x_1 = \frac{M_1}{a_1}.$$

The second chord to be considered is that bounded by the circle $(x-g)^2 + y^2 = V^2$ and the line $x = f$. We note that the chord is at a horizontal distance of $g-f$ from the center. Thus the area of the second chord is the same as the first with R replaced by S and f by $g-f$, so

$$a_2 = \frac{\pi V^2}{2} - (g-f)\sqrt{V^2 - (g-f)^2} - V^2 \sin^{-1} \frac{g-f}{V}.$$

Similarly

$$M_2 = ga_2 - \frac{2}{3} (V^2 - (g-f)^2)^{3/2}.$$

So the x -coordinate of the centroid of the second chord is

$$x_2 = \frac{M_2}{a_2}.$$

Finally the centroid of the region bounded by the two chords is $(x, 0)$, where

$$x = \frac{M_1 + M_2}{a_1 + a_2} \tag{8}$$

Note that when $V = F$, $f = g/2$ and $x = ga_1/2a_1 = g/2$ as expected.

The circle centered at $(0,0)$ and radius F in the analysis corresponds to the outer edge of annulus $n - k$ and the circle centered at $(g,0)$ corresponds to the circle centered at the source with a radius of r_{n-k} (see Figure 1(b)). When the source first transmits a data packet, r_{n-1} is equal to R and F is equal to $(n-1)R$. For a source located at two hops away from D (n equals to two), $F = r_1 = R$, and the centroid is located at $(g/2, 0)$. For any value of n greater than two, F is larger than r_{n-1} , implying that the centroid is located closer to point $(g,0)$ than to point $(0,0)$ within region I_{n-1} . This corresponds to an average penetration factor that is less than one half of R . We can generalize this reasoning to state that the centroid of I_{n-k} is: closer to the source if $r_{n-k} < F$; closer to the destination if $r_{n-k} > F$; and equidistant from both source and destination if $r_{n-k} = F$. In large networks corresponding to a high value of n , the ratio of F to r_{n-k} is higher and the centroid shift from $(g/2, 0)$ towards $(g, 0)$ within the region I_{n-k} is greater. This yields smaller penetration factors for sources at a high hop zones from the destination.

A.2 Transmission Coverage area

The justification for the larger transmission coverage area for smaller n is as follows. Referring again to Figure 15, for a sufficiently large n , a node transmission at distance 0.99 in hop zone n covers a region with area a_1 of almost a semi-circular shape, corresponding to a circle with radius R . The large value of n yields an area a_2 that is almost nil, because the outer arc of annulus n is almost flat. For small values of n , a node transmission at distance 0.99 in zone n covers the same semi-circular region of area a_1 plus a lune of radius of $n - 1$, yielding a larger area a_2 . The smaller the value of n , the larger the area a_2 of this lune, as the results in Figure 6(b) confirm.

REFERENCES

- 802.15.4, I. October 2003. Local and metropolitan area networks: Part 15.4: Wireless medium access control (mac) and physical layer (phy) specifications for low-rate wireless personal area networks (lr-wpans).
- AKKAYA, K. AND YOUNIS, M. 2005. A survey on routing protocols for wireless sensor networks. *Elsevier Journal on Ad Hoc Networks* 3, 3 (May), 325–349.
- ALONSO, J., DUNKELS, A., , AND VOIGT, T. 2006. Bounds on the energy consumption of routings in wireless sensor networks. In *Second Int'l Workshop on Modeling and Optimization in Mobile, Ad-Hoc and Wireless Networks, Cambridge, UK*. IEEE, Cambridge, UK.
- BASU, P. AND REDI, J. 2004. Effect of overhearing transmissions on energy efficiency in dense sensor networks. In *IPSN '04: Proceedings of the third international symposium on Information Processing in Sensor Networks*. ACM Press, New York, NY, USA, 196–204.
- BRAGINSKY, D. AND ESTRIN, D. 2002. Rumor routing algorithm for sensor networks. In *WSNA '02: Proceedings of the 1st ACM international workshop on Wireless Sensor Networks and Applications*. ACM Press, New York, NY, USA, 22–31.
- CERPA, A., BUSEK, N., AND ESTRIN, D. 2005. Scale: A tool for simple connectivity assessment in lossy environments. Tech. rep., in CENS Technical Report 21. September.
- CHIPCON. 2005. CC2420 datasheet. Tech. rep., Chipcon AS, Oslo, Norway.
- DAM, T. V. AND LANGENDOEN, K. 2003. An adaptive energy efficient mac protocol for wireless sensor networks. *ACM Sensys*, 171–180.
- DAS, S. R., PERKINS, C. E., ROYER, E. M., AND MARINA, M. K. 2001. Performance comparison of two on-demand routing protocols for ad hoc networks. *IEEE Personal Communications Magazine special issue on Ad hoc Networking, February 2001* 10, 5, 16–28.

- EL-HOYDI, A. AND DECOTIGNIE, J. 2004. Wisemac: an ultra low power mac protocol for the downlink of infrastructure wireless sensor networks. *Ninth International Symposium on Computers and Communications, 2004. Proceedings. ISCC, Alexandria, EGYPT, June 28 - July 1* 1, 244–251.
- EREN, T., GOLDENBERG, D., WHITLEY, W., YANG, Y., MORSE, A., ANDERSON, B., AND BELHEUMER, P. 2004. Rigidity, computation, and randomization of network localization. *Proc. IEEE Conf. Computer Comm. (Infocom '04)*, 2673–2684.
- GONZALEZ-VELAZQUEZ, A. E., SACKS, L. E., AND MARSHALL, I. W. 2002. Simple Spontaneous Mechanism for Flexible Data Communication in Wireless Ad-hoc Sensor Networks. In *Proceedings of LCS*. Springer.
- HALKES, G. P., VAN DAM, T., AND LANGENDOEN, K. G. 2005. Comparing energy-saving mac protocols for wireless sensor networks. *Mob. Netw. Appl.* 10, 5, 783–791.
- HE, T., BLUM, B. M., STANKOVIC, J. A., AND ABDELZAHER, T. 2004. Aida: Adaptive application-independent data aggregation in wireless sensor networks. *Trans. on Embedded Computing Sys.* 3, 2, 426–457.
- INTANAGONWIWAT, C., GOVINDAN, R., AND ESTRIN, D. 2000. Directed diffusion: a scalable and robust communication paradigm for sensor networks. In *Mobile Computing and Networking*. ACM, Boston, MA, 56–67.
- INTANAGONWIWAT, C., GOVINDAN, R., ESTRIN, D., HEIDEMANN, J., AND SILVA, F. 2003. Directed diffusion for wireless sensor networking. *IEEE/ACM Trans. Netw.* 11, 1, 2–16.
- JOHNSON, D. AND MALTZ, D. 1996. Dynamic source routing in ad hoc wireless networks. *Mobile Computing* 353, 153–181.
- JURDAK, R. 2007. *Wireless Ad Hoc and Sensor Networks: A Cross-Layer Design Perspective*. Springer-Verlag, New York, NY, USA.
- JURDAK, R., BALDI, P., AND LOPES, C. V. 2007. Adaptive low power listening for wireless sensor networks. *IEEE Transaction on Mobile Computing* 6, 8 (August), 988–1004.
- JURDAK, R., LOPES, C. V., AND BALDI, P. 2006. *Battery Life Estimation and Optimization for Underwater Sensor Networks*. Sensor Network Operations. IEEE-Wiley, Hoboken, NJ, USA, Chapter 6, 397–420.
- KARP, B. AND KUNG, H. T. 2000. Gpsr: greedy perimeter stateless routing for wireless networks. In *MobiCom '00: Proceedings of the 6th annual international conference on Mobile Computing and Networking*. ACM Press, New York, NY, USA, 243–254.
- KAWADIA, V. AND KUMAR, P. R. 2005. A cautionary perspective on cross-layer design. *Wireless Communications* 2, 3–11.
- KRISHNAMACHARI, B., ESTRIN, D., AND WICKER, S. 2002. Modelling data-centric routing in wireless sensor networks. in *Proc. of the 2002 IEEE INFOCOM'02*.
- LU, G., KRISHNAMACHARI, B., AND RAGHAVENDRA, C. S. 2004. An adaptive energy-efficient and low-latency mac for data gathering in sensor networks. In *In proc. of International workshop on Algorithms for Wireless, Mobile, ad Hoc Sensor Networks*. IEEE Computer Society, Denver, CO, USA.
- MARÓTI, M. 2004. Directed flood-routing framework for wireless sensor networks. In *Middleware '04: Proceedings of the 5th ACM/IFIP/USENIX international conference on Middleware*. Springer-Verlag New York, Inc., New York, NY, USA, 99–114.
- MELODIA, T., VURAN, M. C., AND POMPILI, D. 2005. The State of the Art in Cross-layer Design for Wireless Sensor Networks. In *Proceedings of EuroNGI Workshops on Wireless and Mobility*. Springer Lecture Notes in Computer Science 3883. Como, Italy, 78–92.
- MOORE, D., LEONARD, J., RUS, D., AND TELLER, S. 2004. Robust distributed network localization with noisy range measurements. In *SenSys '04: Proceedings of the 2nd international conference on Embedded Networked Sensor Systems*. ACM Press, New York, NY, USA, 50–61.
- PARK, V. D. AND CORSON, M. S. 1997. A highly adaptive distributed routing algorithm for mobile wireless networks. In *INFOCOM '97. Sixteenth Annual Joint Conference of the IEEE Computer and Communications Societies*. INFOCOM. IEEE, Kobe, Japan, 1405–1413.

- PERKINS, C. AND ROYER, E. 1999. Ad-hoc on-demand distance vector routing. In *WMCSA '99: Proceedings of the Second IEEE Workshop on Mobile Computer Systems and Applications*. IEEE, Washington, DC, USA, 90.
- POLASTRE, J., HILL, J., AND CULLER, D. 2004. Versatile low power media access for wireless sensor networks. In *In proceedings of the 2nd international conference on Embedded Networked Sensor Systems, SenSys*. ACM Press, Baltimore, MD, USA, 95–107.
- POLASTRE, J., HUI, J., LEVIS, P., ZHAO, J., CULLER, D., SHENKER, S., AND STOICA, I. 2005. A unifying link abstraction for wireless sensor networks. In *SenSys '05: Proceedings of the 3rd international conference on Embedded networked sensor systems*. ACM, New York, NY, USA, 76–89.
- POLASTRE, J., KARLOF, C., AND LI, Y. 2003. Arrive: Algorithm for robust routing in volatile environments. Tech. Rep. UCB//CSD-03-1233, University of California at Berkeley. March.
- RANGWALA, S., GUMMADI, R., GOVINDAN, R., AND PSOUNIS, K. 2006. Interference-aware fair rate control in wireless sensor networks. *SIGCOMM Comput. Commun. Rev.* 36, 4, 63–74.
- RHEE, I., WARRIER, A., AIA, M., AND MIN, J. 2005. Z-mac: a hybrid mac for wireless sensor networks. In *In proc. of the 3rd international conference on Embedded Networked Sensor Systems, Sensys05*. ACM Press, New York, USA, 90–101.
- RUZZELLI, A., O'HARE, G., AND JURDAK, R. 2008. Merlin: Cross-layer integration mac and routing for low duty-cycle sensor networks. *Elsevier journal Ad Hoc Networks* 6, 4.
- RUZZELLI, A., O'HARE, G., O'GRADY, M., AND TYNAN, R. 2006. Merlin: A synergetic integration of mac and routing protocol for distributed sensor networks. In *proceeding of Third Annual IEEE Communication Society Conference on Sensor, Mesh and Ad Hoc Communications and Networks (SECON 2006), Reston, VA, USA*, 266–275.
- SRINIVASAN, K., DUTTA, P., TAVAKOLI, A., AND LEVIS, P. 2006. Some implications of low-power wireless to ip routing. In *Proc. of the Fifth Workshop on Hot Topics in Networks HotNets V*. Irvine, CA, USA.
- TSENG, Y.-C., NI, S.-Y., Y-S., C., AND SHEU, J.-P. March 2002. The broadcast storm problem in a mobile ad hoc network. *Wireless Networks* 8, 153–167(15).
- UCBERKELEY. Minroute routing protocol.
- WILLIAMS, B. AND CAMP, T. 2002. Comparison of broadcasting techniques for mobile ad hoc networks. In *MobiHoc '02: Proceedings of the 3rd ACM international symposium on Mobile Ad Hoc Networking & Computing*. ACM Press, New York, NY, USA, 194–205.
- WOO, A., TONG, T., AND CULLER, D. 2003. Taming the underlying challenges of reliable multihop routing in sensor networks. In *SenSys '03: Proceedings of the 1st international conference on Embedded Networked Sensor Systems*. ACM, New York, NY, USA, 14–27.
- WU, J., HAVINGA, P., DULMAN, S., AND NIEBERG, T. 2004. Eyes source routing protocol for wireless sensor networks. *Proc. of European Workshop on Wireless Sensor Networks EWSN*, 67–70.
- YE, F., CHEN, A., LIU, S., AND ZHANG, L. 2001. A scalable solution to minimum cost forwarding in large sensor networks. *Proceedings of Tenth International Conference on Computer Communications and Networks, Pages 304 -309*.
- YE, W., HEIDEMANN, J., AND ESTRIN, D. 2004. Medium access control with coordinated adaptive sleeping for wireless sensor networks. *IEEE/ACM Transactions on Networking* 3, 1567–1576.
- ZHAO, J. AND GOVINDAN, R. 2003. Understanding packet delivery performance in dense wireless sensor networks. In *SenSys '03: Proceedings of the 1st international conference on Embedded Networked Sensor Systems*. ACM Press, New York, NY, USA, 1–13.
- ZHOU, G., HE, T., KRISHNAMURTHY, S., AND STANKOVIC, J. A. 2004. Impact of radio irregularity on wireless sensor networks. In *MobiSys '04: Proceedings of the 2nd international conference on Mobile systems, applications, and services*. ACM Press, New York, NY, USA, 125–138.
- ZORZI, M. AND RAO, R. R. 2003. Geographic random forwarding (gegraf) for ad hoc and sensor networks: Multihop performance. *IEEE Transactions on Mobile Computing* 2, 4, 337–348.